J Mater Sci: Mater Electron (2008) 19:457–462
DOI 10.1007/s10854-007-9362-x

# Electrical properties of electrodeposited polyaniline nanotubes

**Edson Giuliani R. Fernandes · Demetrio Artur W. Soares · Alvaro Antonio Alencar De Queiroz**

Received: 26 February 2007 / Accepted: 26 June 2007 / Published online: 2 August 2007
© Springer Science+Business Media, LLC 2007

**Abstract** The electrical properties of polyaniline nanotubes-aluminum like Schottky diode are described. Polyaniline nanotubes (PANI) were deposited on aluminum thin films using the polarographic technique. The nanotubes were characterized by scanning electron microscopy (SEM) and UV-Vis absorption spectra. The electrical properties of the heterojunction PANI-Al were examined. The current density–voltage ($J \times$ V) profile has shown a behavior typical of Schottky diode, with ideality factor (n) of 6.76 and $\phi_b$ of 0.70 eV. Impedance spectroscopy data apparently shows that the resistance dominated the AC behavior of the PANI-Al system. The equivalent circuit is composed from a resistor in series with a parallel resistor–capacitor circuit. The results indicate that polyaniline nanotubes may be interesting to the development of electro-optical devices with 2D structure.

## 1 Introduction

The semi-conducting property of polyaniline has over the last few decades been explored as the active material in a number of electronic and electrochemical devices. Polyaniline may be generally solution processable, which makes it possible to manufacture devices on flexible carriers, ultimately at a very low cost with common printing techniques [1].

The recent development of nanoscience and nanotechnology has opened up novel fundamental and applied frontiers in surface functionalization and characterization. At the nanometer scale, the high surface-to-volume ratio characteristic of most nanomaterials has been demonstrated to have a tremendous influence of many fundamental material properties and electro-optical device performance [2–4].

In the last two decades the studies on polymer-metal heterojunctions (PMH's) have lead a great relevance in the optoelectrochromic area due to the project of electrochromic devices, field effect transistors (FET's), supercapacitors, an more else [5]. The principal physical chemical characteristics of these materials are the easily processing, low cost and nonlinear properties of the device [6].

The possibility of obtaining nanostrucurated PMH's surface is attractive, since it is possible to produce materials whose electrical characteristics can be topologically modulated.

A particularly interesting PMH for the nanodevices project involves the synthesis of polymer conjugated-metal type interfaces. In this case, polyaniline has attracted considerable interest due its good environmental stability.

Recently, heterojunctions obtained from polyaniline nanostructures (PANI) has become an interest of our laboratory [7, 8]. In particular the electrical properties and Schottky barriers devised with nanostrucurated polyaniline it is a great of interest. In this paper, we report the junction characteristics between p-type (anion-doped) PANI and Al thin films.

E. G. R. Fernandes · D. A. W. Soares ·
A. A. A. De Queiroz (✉)
Departamento de Física e Química, Instituto de Ciências Exatas-Universidade Federal de Itajubá (UNIFEI),
Av. BPS 1303, Itajuba, MG, 37500-903, Brazil
e-mail: alencar@cpd.efei.br

## 2 Experimental

### 2.1 The PANI-Al heterojunction

Protonated polyaniline nanotubes (PANI) was polarographicaly deposited at thin aluminum films (Alcoa, 99.99%, 30.0 µm, 2 V) in solution containing aniline

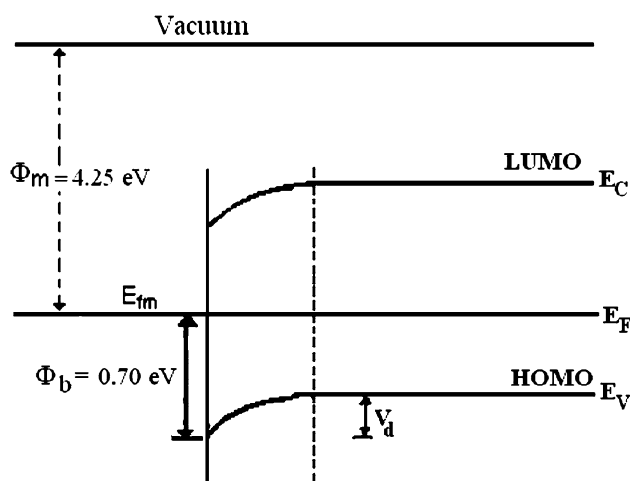


**Scheme 1** Schematic diagram of the PANI-Al heterojunction at zero potential

(Sigma-Aldrich, 99.0%, 2.2 mM) and $H_2SO_4$ (Merck, 1 M) at room temperature (27 °C). The PANI-Al schematic diagram at zero bias is shown in Scheme 1. An ohmic contact with the PANI layer for the electrical measurements was formed by Ag (Siemens 99.99%, paste) having a high work function (6.35 eV).

### 2.2 Characterization of electrodeposited PANI

The electrodeposited PANI nanotubes were characterized by scanning electron microscopy (SEM) on a Phillips, XL30. The protonation of the PANI was confirmed by the UV/Vis spectroscopy carried out on a Varian 634 spectrophotometer. The PANI electrodeposited at aluminum surface was dissolved in N-methylpyrrolidone (NMP) for the UV/Vis analysis. The electrical properties of the PANI-Al heterojunction were studied by $J \times$ V analysis using an electrometer Keithley (K237) and impedance analysis using a LCR Precision Meter (HP4284A) with variance of 20–1 MHz. The resistive characteristics of the polyaniline nanotubes were estimated by 4-probe configuration. The Scheme 2 shows the PANI-Al configuration to the electrical measurements ($J \times$ V and AC curves).

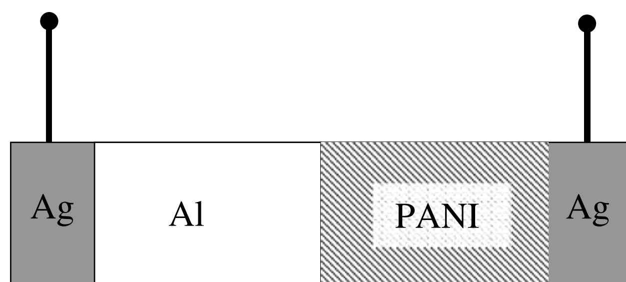


**Scheme 2** Schematic of the PANI-Al configuration for the electrical measurements ($J \times$ V and AC curves)

## 3 Results and discussion

The microstructural analysis SEM (Fig. 1) shows the PANI nanotubes obtained in this work. The mechanism of nanotubes formation seems to involve an initial nucleation into microcavities taking the shape as a result of the oxidation process in the metal Al film. In this case, the nanotubes formation is due the aluminum nucleation of aniline molecules into the aluminum formed pores (Fig. 1 B), when a pite oxidation takes place. Then, the polymerization proceeds with increment of new aniline molecules that can interact with each other, through the amine and iminium nitrogen interaction, to form at the same time a fibrous PANI nanostructure.

Removing the polymer coating, the substrate appeared white in coloration evidencing the thick $Al_2O_3$ oxide formation (a passive layer that protects the Al metal from corrosion, once the PANI electrodeposition was made in a corrosive ambient).

The absorbance UV/Vis spectroscopic analysis of the synthesized PANI nanotubes is shown in Fig. 2. The band at 295 nm present in the spectrum corresponds to the pernigraniline totally oxidation state, and it is associated with the $\pi - \pi^*$ transition [9]. The band at 430 nm corresponds to partial oxidation of PANI and can be assigned to represent the intermediate state between leucoemeraldine form containing benzenoid rings and emeraldine form containing conjugated quinoid rings in the main chain of the PANI [10]. The last band at 610 nm is assigned to exciton formation in the quinonoid rings [11].

The band-gap energy of the polymer may be estimated using the relation [12]

$$\alpha = (2.3003A) = K\left(h\upsilon - E_g\right)^{1/2} \quad (1)$$

where $\alpha$ is the absorption coefficient, A is the absorbance, and K is an empirical constant that is proportional to the thickness deposited polymer. The h$\nu$ and $E_g$ are the photon energy and the energy band-gap, respectively. Plotting $\alpha^2$ versus h$\nu$ (inset in Fig. 2) gives a straight line whose intercept on the abscissa is the band gap energy. The $E_g$ value was estimated to be 3.3 eV, in according to the literature values [13].

The $J \times$ V curve for the system PANI-Al is shown in Fig. 3. The curve is asymmetric and non-linear indicating a rectifying character of the PANI-Al heterojunction. Thus, polarizing negatively the metal with respect to the PANI the forward current increases exponentially in the lower-voltage region and increase linearly in the higher-voltage region, presenting an electrical Schottky diode behavior characteristic. In this case, the operating voltage is typically equal, or lower than, the semiconductor band-gap.

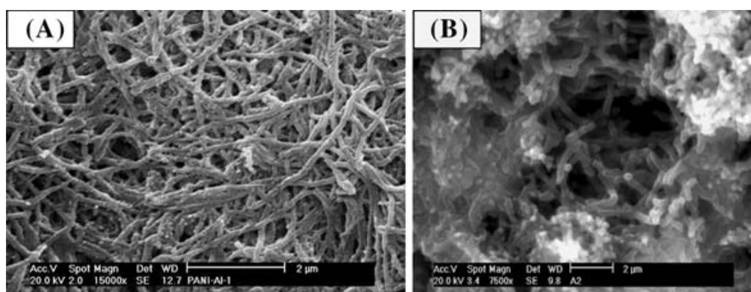


**Fig. 1** SEM micrograph of the PANI nanotubes (**A**) and nucleation process into pores (**B**)

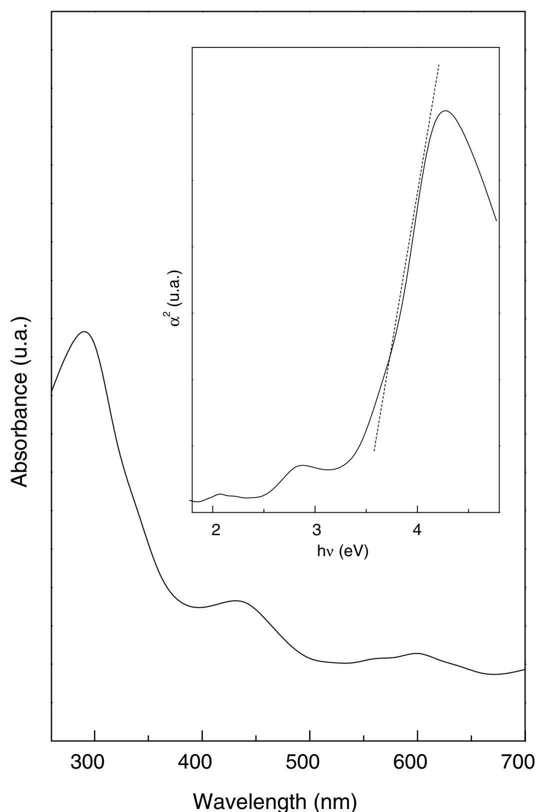


**Fig. 2** Optical absorption spectrum of doped PANI. Inset: Curve used for the calculus of the band gap energy ($E_g$). Temperature: 27 °C

The behavior like Schottky diode, unbecoming of the polymeric materials, is due to the interface semiconductor (PANI)-metal (Al). It is very known fact that the Fermi levels ($E_F$) are different in the metal-polymer interface. Once the electrons are the only carrier of charges, the balance donor-receiver is only reached when the $E_F$ levels in the semiconductor and in the metal they join through a flow of carriers of the metal for the semiconductor. A depletion layer is then formed, leading a reduction of the energy band and the formation of Schottky barrier [14] that it is opposed to an additional electronic flow. This behavior checks the heterojunction PANI-Al a rectifier character, as showed in the Fig. 3. The behavior of the current density per area unit ($J$) as an applied voltage function (V) can be expressed as

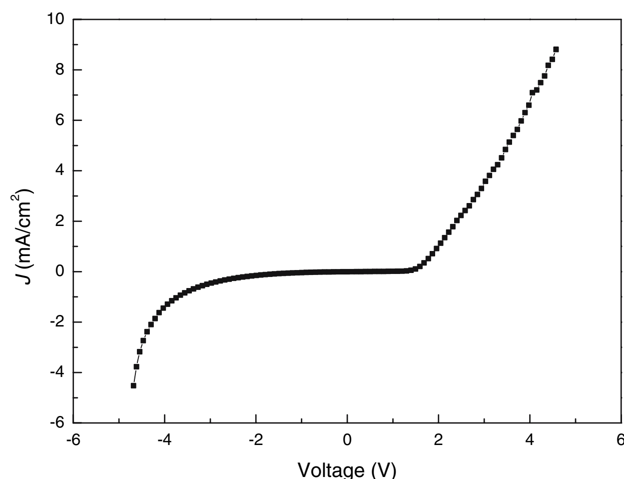


**Fig. 3** Current density versus applied voltage ($J \times$ V) for the PANI-Al heterojunction

$$J = J_0[\exp(\mathrm{eV/nkT}) - 1] \tag{2}$$

where $J_0$ is the saturation current density, e is the electronic charge, k is the Boltzmann constant, T is the absolute temperature and n is the ideality factor (for an ideal diode n = 1).

The current becomes linear at a forward bias voltage greater than 1.4 V, suggesting that the bulk resistance of the PANI in this voltage region dominates the device resistivity. Therefore, the slope of the mentioned region estimates the bulk conductivity to be 1.02 mS $\cdot$ cm$^{-1}$.

The ideality factor (n) and the reverse saturation current density ($J_0$) for the PANI-Al can be calculated from the gradient Ln ($J$) $\times$ V through linearization of the Eq. (2) considering $eV/kT \gg 1$ (Fig. 4). Using the best-fit line equation, the ideality factor was calculated resulting in n = 6.76 and $J_0 = 1.98 \times 10^{-5}$ (A $\cdot$ cm$^{-2}$).

The barrier height $\phi_b$ can be deduced using the Richardson equation

$$J_0 = \mathrm{A^*T^2} \exp[-e\phi_b/\mathrm{kT}] \tag{3}$$

where A* is the effective Richardson constant usually taken as 120 A $\cdot$ cm$^{-2}$ $\cdot$ k$^{-2}$ [15]. The value for the barrier height is estimated to be $\phi_b$ = 0.70 (eV).

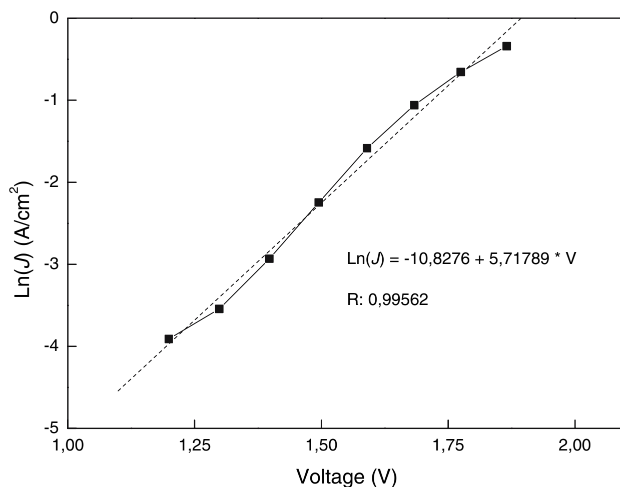


**Fig. 4** Ln($J$) × V characteristic of the PANI-Al heterojunction

The existence of surface states reduces significantly the value of the ideality factor of the device. By the calculation of the n value through $J \times$ V curve supply the value n = 6.76. The ideality deviation can be result as an elevated grade of imperfections on the PANI-Al heterojunction and/or due the presence of an interfacial layer, resulting in a great number of superficial states localized in the band-gap, influencing in the height of Schottky barrier.

The electrical conductivity at 27 °C for the deposited film, using the 4-probe method, was about 10 mS · $cm^{-1}$, near of the germanium, an inorganic semiconductor of current use in the electronic industries.

Another phenomena for the metal-polymer diode devices discussed in the light of Schottky emission is the Poole–Frenkel emission, associated with the material bulk barriers (Acceptor and donor sites, traps, or electrons in the valence band), and the space-charge limited current (SCLC), associated with the traps at the interfacial region between metal and polymer [15, 16].

The current density for Poole–Frenkel emission can be expressed by the following equation:

$$J/V = (J_0/V_0)\exp[\beta(\mathrm{V/d})^{1/2}/\mathrm{nkT}] \quad (4)$$

where d is the thickness of the polymer coating and $\beta = (\mathrm{e}^3/\pi\varepsilon\varepsilon_0)^{1/2}$ in which ε is the dielectric constant of the polymer and $\varepsilon_0$ is the free-space permittivity.

The SCLC conduction mechanism is given by:

$$J = [(8\varepsilon\varepsilon_0\mu \mathrm{V}^2)/(9\mathrm{d}^3)] \propto \mathrm{V}^2 \quad (5)$$

where $\mu$ is the carrier mobility.

A Ln($J$/V) × $V^{1/2}$ plot and Log ($J$) × Log (V) plot should give a linear curve in the Poole–Frenkel emission case or SCLC conduction mechanism, respectively. In the last case, a slope of 2 is expected.

In this work it was observed that the Poole–Frenkel and SCLC plot not give a straight line for the PANI-Al junction, thus ruling out the Poole–Frenkel or SCLC emission mechanism. Therefore it is inferred that Schottky emission is the major mechanism in the PANI-Al device. However, we cannot eliminate the tunneling mechanism, since the $J \times$ V curve also shows quite satisfactory linearity in Fowler-Nordheim (Ln(1/V) ∝ 1/V) coordinates (Fig. 5). Thus, tunneling process may be equally as important in these devices as the thermionic emission process.

The impedance spectroscopy (Nyquist diagram) study for the electrodeposited PANI is represented in Fig. 6. The correspondent AC impedance curve is a semi-circle, which can be expressed by the equivalent circuit shown in Fig. 7. In the circuit, $R_b$ is the resistance inside the conducting layer, $R_{dl}$ is a resistance of the non-conducting part of the material and $C_{dl}$ is the double layer capacitance caused by the thin aluminum oxide film ($Al_2O_3$) formed during the electrodeposition process. The estimate value for $C_{dl}$ and $R_b$ can be estimated by using the relationships $C_{dl} = 1/(2\pi f_{max} R_{dl})$ and $R_{DC} = R_{dl} + R_b$, $f_{max}$ being the frequency at the top of the semi-circle (Fig. 6), $R_{dl}$ the diameter of the semi-circle and $R_{DC}$ the measured 4-probe resistance [17]. The related parameters for the PANI are: $C_{dl} \approx 10$ μF,

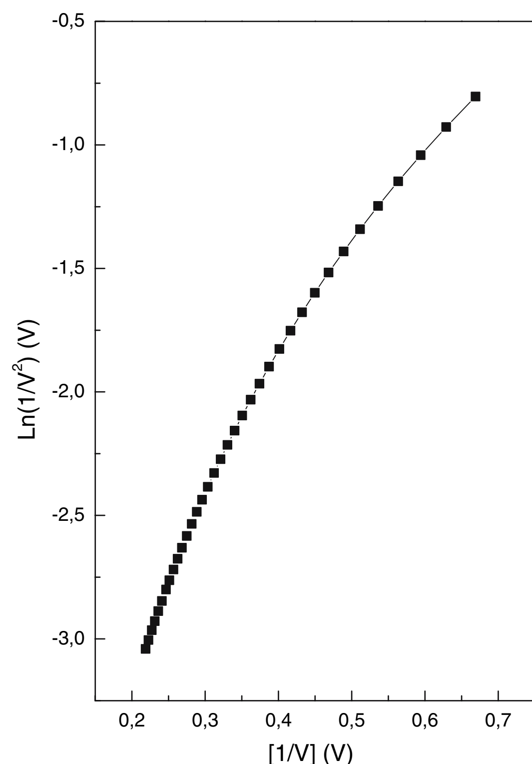


**Fig. 5** Ln($1/V^2$) × 1/V plot (Fowler-Nordheim tunneling mechanism) for PANI-Al. $R^2$ = 0.9975 for 1/V > 0.4, and $R^2$ = 0.9970 for 1/V < 0.4

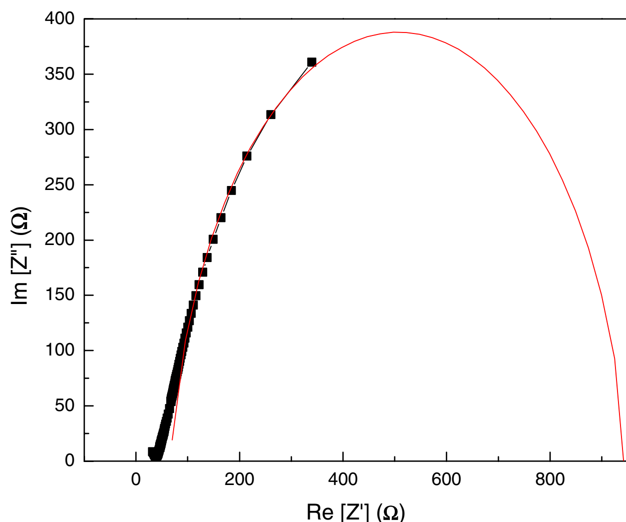


**Fig. 6** Nyquist plot for the PANI-Al heterojunction

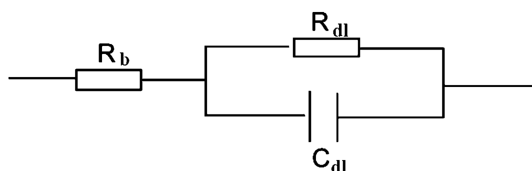


**Fig. 7** The equivalent circuits for a semi-circle Nyquist plot

$R_{dl} \approx 822\ \Omega$ and $R_b \approx 97\ \Omega$ (approximately equals to the estimated bulk conductivity using the Fig. 3 (90 Ω)).

The frequency real part dependence of the PANI-Al impedance is shown in Fig. 8 and Bode plot is represented in Fig. 9. The real part of the impedance is starting to decrease even from low frequencies, being this effect determined by the double layer capacitance of the equivalent circuit. At low frequencies, the phase shift is negligible confirming the simple circuit.

The impedance spectroscopy studies indicate that the resistance dominates the ac behavior of the heterojunction PANI-Al [18].

## 4 Conclusions

Heterojunctions of the type polymer-metal were obtained by the polarograthic deposition of PANI nanotubes in Al. The analysis of the $J \times V$ and $\mathrm{Ln}(J/V) \times V^{1/2}$ data indicate that the PANI/Al heterojunction possess an Schottky diode behavior with thermally emission as the major mechanism., with $n = 6.76$, $\phi_b = 0.70$ (eV) and $J_0 = 1.98 \times 10^{-5}$ (A · cm$^{-2}$). The related AC behavior parameters obtained with the equivalent circuit (a resistor in series with a parallel resistor–capacitor) for the PANI-Al systems are: $C_{dl} \approx 10\ \mu F$, $R_{dl} \approx 822\ \Omega$ and $R_b \approx 97\ \Omega$. The bulk resistance obtained with the AC behavior is in agreement with the estimated bulk resistance obtained by DC studies (4-probe and $J \times V$ curve).

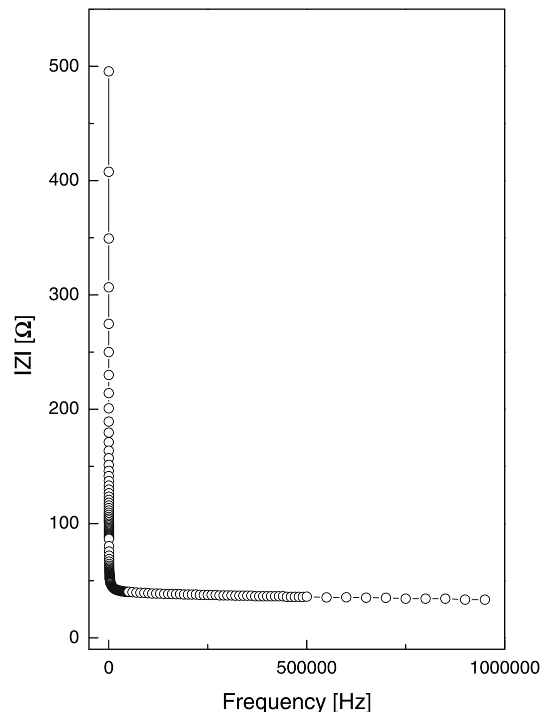


**Fig. 8** Dependence of the impedance module with the frequency for PANI electrodeposited at Al thin film

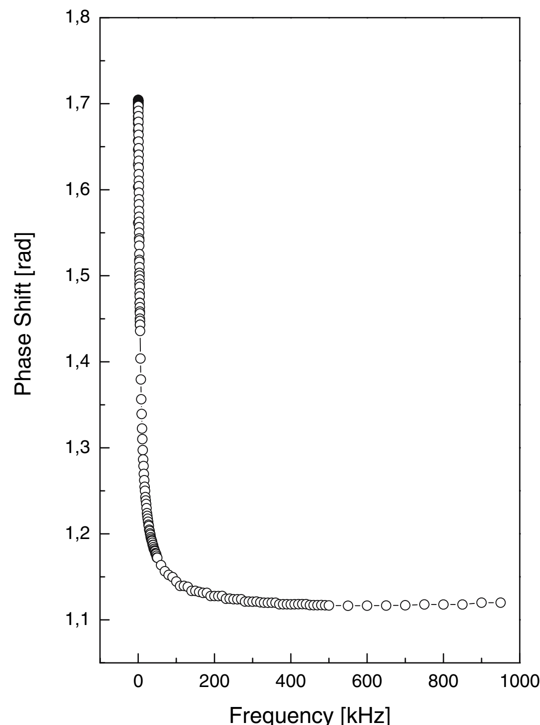


**Fig. 9** Bode plot for the PANI-Al heterojunction

**Acknowledgement** The authors are grateful to CNPq for the partial financial support of this work.

## References

1. H.E. Katz, Chem. Mater. **16**, 4748 (2004)
2. E.G.R. Fernandes, A.A.A. Queiroz, G.A. Abraham, J. San Román, J. Mat. Sc. Mat. Med. **17**, 105 (2006)
3. L. Dauginet-De Pra, S. Demoustier-Champagne, Thin Sol. Fil. **479**, 321 (2005)
4. G.B. Blanchet, Y.-L. Loo, J.A. Rogers, F. Gao, C.R. Fincher, Appl. Phys. Lett. **82**, 463 (2003)
5. R.M. Faria, O.N. Oliveira Jr., Bras. J. Phys. Org. Chem. **61**, 4439 (1996)
6. A. Pron, P. Rannou, Prog. Polym. Sci. **27**, 135 (2002)
7. E.G.R. Fernandes, D.A.W. Soares, A.A.A. Queiroz, in *8° Congresso Brasileiro de Polímeros, Águas de Lindóia*, 99 (2005)
8. E.G.R. Fernandes, D.A.W. Soares; A.A.A. Queiroz, in *IV Encontro da Sociedade Brasileira de Materiais, Recife*, 53 (2005)
9. J.E. De Albuquerque, L.H.C. Mattoso, R.M. Faria, J.G. Masters, A.G. Macdiarmid, Synth. Met. **146**, 1 (2004)
10. T. Lindfors, C. Kvarnström, A. Ivaska, J. Electroanal. Chem. **5218**, 131 (2002)
11. K.G. Conroy, C.B. Breslin, Electrochem. Acta. **48**, 721 (2003)
12. L.-M. Huang, T.-C. Wen, A. Gopalan, F. Ren, Mat. Sci. Eng. B **104**, 88 (2003)
13. R.K. Gupta, R.A. Singh, Compos. Sci. Technol. **65**, 677 (2005)
14. W. Schottky, Z. Phys. **15**, 872 (1914)
15. M. Sze. *Physics of Semiconductor Devices*. (John Wiley & Sons, New York, 1972)
16. H. Frenkel, Phys. Rev. **54**, 647 (1938)
17. P. Passiniemi, K. Väkiparta, Synht. Met **69**, 237 (1995)
18. D. Hui, R. Alexandrescu, M. Chipara, I. Morjan, G.H. Abdica, M.D. Chipara, K.T. Lau, J. Opt. Adv. Mat. **6**, 817 (2004)